Arginine 719 in Human Plasminogen Mediates Formation of the Staphylokinase:Plasmin Activator Complex†

Laurent Jespers,*,‡ Nathalie Van Herzeele,‡ H. Roger Lijnen,§ Berthe Van Hoef,§ Marc De Maeyer,‡ Désiré Collen,‡,§ and Ignace Lasters‡

Center for Transgene Technology and Gene Therapy, Flanders Interuniversity Institute for Biotechnology, and Center for Molecular and Vascular Biology, KULeuven, Leuven, Belgium

Received November 17, 1997; Revised Manuscript Received February 18, 1998

ABSTRACT: Staphylokinase (Sak), a 16-kDa bacterial protein, forms a 1:1 stoichiometric complex with the serine proteinase domain of human plasmin, which in turn converts other plasminogen molecules into plasmin. To identify amino acid residues critical for generating the Sak:plasmin activator complex, alanine-scanning mutagenesis was performed on phage-displayed micro-plasminogen (μPlg). Substitution of Arg719 with Ala [μPlg(R719A)] disrupted complex formation, although the sensitivity of phage-displayed μPlg(R719A) to activation by urokinase and the amidolytic activity of the micro-plasmin derivative [μPli-(R719A)] remained unaffected. Likewise, the soluble μPlg(R719A) molecule did not generate a functional activator complex with Sak, whereas quantitative activation into plasmin was obtained upon incubation with either urokinase or the Sak:plasmin complex. Real-time biospecific affinity measurements revealed that the Arg → Ala substitution at position 719 increased the equilibrium dissociation constant between μPlg(R719A) and Sak from 46 nM to 1 μM, primarily by reducing the association rate constant. Arg719 has recently also been implied in the functional complex formation between human plasmin and streptokinase [Dawson, K. M., Marshall, J. M., Raper, R. H., Gilbert, R. J., and Ponting, C. P. (1994) *Biochemistry 33,* 12042−12047.], suggesting that both bacterial cofactors may share common structural and/or mechanistic aspects for plasminogen activation.

Plasmin (Pli)[1] is an 85-kDa serine proteinase which plays a central role in hemostasis by degrading fibrin clots into soluble degradation products (*1*). In human plasma, it circulates as a proenzyme, plasminogen (Plg), which is activated by proteolytic cleavage of the Arg561−Val562 peptide bond by tissue-type plasminogen activator or urokinase. Human Plg can also be activated by two bacterial proteins, streptokinase (SK) (*2, 3*) and staphylokinase (Sak) (*4, 5*). Unlike tissue-type plasminogen activator and urokinase, the bacterial plasminogen activators are devoid of serine proteinase activity but form tight 1:1 stoichiometric complexes with Pli, which as a result, exhibit Plg activation potential. It is believed that, upon binding of Sak (reviewed in *6*) or SK (*7*) to Pli, the conformation of the active site is altered such that the proteinase moiety of the complex can recognize and activate other substrate molecules of Plg into Pli by selective cleavage of the same Arg−Val peptide bond. While both Sak and SK modify the substrate specificity of Pli, SK also induces Plg activation ability in the Plg molecule. Here, binding of SK to the proenzyme results in the formation of a reversible proteolytic active site ("virgin" enzyme) without conversion of Plg into double-chain Pli (*7, 8*).

Sak and SK differ also with respect to their interactions with the physiological Pli inhibitor, α_2-antiplasmin (*9*−*11*). In contrast to the SK:Plg complex, the Sak:Pli complex is rapidly neutralized in plasma in the absence of fibrin, thereby avoiding systemic Plg activation and the breakdown of circulating fibrinogen. Despite these differences, the similar enzymatic properties of the SK:Pli and Sak:Pli complexes suggest that these two indirect plasminogen activators may share common structural features which determine their

† This work was supported in part by a sponsored research agreement between the Flemish Institute for the Advancement of Scientific and Technological Research in the Industry (IWT) and Thromb-X NV, a spin-off company of the University of Leuven, in which D. Collen has an equity interest.

* Address correspondence to this author: Center for Transgene Technology and Gene Therapy, Flanders Interuniversity Institute for Biotechnology, Campus Gasthuisberg O&N, Herestraat 49, B-3000 Leuven, Belgium. Tel: +32-16-345772 or +32-16-346036. Fax: +32-16-345990. E-mail: laurent.jespers@med.kuleuven.ac.be.

‡ Center for Transgene Technology and Gene Therapy.

§ Center for Molecular and Vascular Biology.

[1] Abbreviations: Plg, human plasminogen; Pli, plasmin (activated human Plg); mPlg, mini-plasminogen (human plasminogen comprising amino acids 444−791); mPli, mini-plasmin (activated human mPlg); μPlg, micro-plasminogen (human plasminogen comprising amino acids 543−791); μPli, micro-plasmin (activated μPlg); μPlg(A#B), micro-plasminogen with amino acid A in position # substituted with amino acid B; Sak, staphylokinase; SK, streptokinase; kDa, kilodalton; pIII, gene *III* product of filamentous phage; S-2403, pyroglutamylphenylalanyllysine *p*-nitroanilide hydrochloride; D-Val-Phe-Lys-CH_2Cl, D-valylphenylalanyllysyl-chloromethane; AEBSF, (aminoethyl)benzenesulfonyl fluoride; SOE, splicing by overlap extension; PCR, polymerase chain reaction; cfu, colony-forming unit; BSA, bovine serum albumin; Tris, tris(hydroxymethyl)aminomethane; TBS, 50 mM Tris-HCl, 140 mM NaCl, pH 7.4; OPD, *o*-phenylene diamine dihydrochloride; LB, Luria-Bertani (medium); IPTG, isopropyl β-D-thiogalactoside; rpm, revolution per min; EDTA, ethylenediaminetetraacetic acid; SDS, sodium dodecyl sulfate; PAGE, polyacrylamide gel electrophoresis; HEPES, *N*-(2-hydroxyethyl)piperazine-*N*′-2-ethanesulfonic acid; k_a, association rate constant; k_d, dissociation rate constant; K_D, apparent dissociation constant. Amino acids are indicated by the standard three- or one-letter abbreviations.

S0006-2960(97)02807-9 CCC: $15.00
Published on Web 04/15/1998

mechanisms of action. Thus, it has been shown that the 28-kDa serine proteinase domain of Pli, micro-plasmin (μPli), is only required for functional complex formation with both bacterial cofactors (*12, 13*). Moreover, Sak and SK compete for binding to Pli, thereby indicating that their respective binding sites on Pli overlap at least partially (*13*).

Most studies on the molecular determinants that mediate Plg activator complex formation have focused on the identification of the functional epitopes on SK and Sak. Mutagenesis of two clusters of charged amino acid residues in Sak (46−50 and 65−69) resulted in a 10- to 20-fold impairment of its interaction with Pli (*14*). In SK, the NH_2-terminal segment (1−59) and a central region (143−293), which were later delineated to segments 37−51, 234−253, and 274−293 by peptide walking analysis, provide Plg-binding ability (*15* and references therein). Interestingly, in both Sak and SK, mutation of several amino acid residues which do not contribute detectably to the free energy of binding to Pli results in a markedly reduced activity for Plg activation (e.g., residues 11, 13, and 14 in Sak, and residues 332 and 334 in SK) (*14, 16*). This may suggest that the respective Pli-binding epitopes are not congruent with the functional epitopes.

The specific structures on Plg that mediate complex formation with these bacterial cofactors are largely unknown, although several recombinant expression systems for soluble Plg or truncated forms thereof have been elaborated (*17*−*20*). Recently, we have developed an alternative expression approach whereby a truncated form of human Plg, micro-plasminogen (μPlg), is functionally displayed on the surface of filamentous phage via a covalent link to the minor coat protein III (pIII) (*21*). For epitope mapping, the phage display system is particularly convenient because of the easy generation of mutants and the rapid production of small amounts of material for biochemical evaluation (*22*).

In the present study, this sytem has been used to search for plasmin residues which are critical in the Sak:Pli interface. Site-directed mutagenesis of nine solvent-exposed residues in μPlg led to the identification of one amino acid, Arg719, of which substitution by Ala strongly reduces the binding affinity and Plg activation potential of the Sak:μPli complex.

EXPERIMENTAL PROCEDURES

Reagents. Oligonucleotides were synthesized at Eurogentec (Belgium). Human Plg and urokinase (two-chain molecule) were prepared as previously described (*23, 24*). Mini-plasminogen (mPlg) and the recombinant Plg mutant S741A [Plg(S741A)] were obtained as described (*25, 26*). The chromogenic substrate S-2403 (pyroglutamylphenylalanyllysine *p*-nitroanilide hydrochloride) was obtained from Chromogenix (Sweden). Human α_2-antiplasmin and recombinant Sak were produced and purified as previously described (*11, 27*). D-Valylphenylalanyllysyl-chloromethane (D-Val-Phe-Lys-CH_2Cl) was synthesized at UCB (Belgium). Murine monoclonal antibody 31E9 directed against mPlg was produced as described previously (*28*). CNBr-activated Sepharose, PD-10 columns, and horseradish peroxidase-conjugated anti-M13 Ig were purchased from Pharmacia (Sweden). (Aminoethyl)benzenesulfonyl fluoride (AEBSF) was obtained from Sigma (Belgium).

Modeling of the Serine Proteinase Domain of Plasmin. The main-chain trace of the serine proteinase domain of plasmin, μPli, was homology modeled using the spare parts approach (*29*) available in the Brugel modeling package, using trypsin as the starting template. Side-chains were added and oriented in their global minimum energy conformation using the dead-end elimination method (*30, 31*).

Construction of the Fmyc-μPlg-5RS vector. The type 3 phage vector Fmyc-μPlg, used for phage display of μPlg by fusion to the NH_2 terminus of pIII (*21*), was redesigned to facilitate the mutagenesis experiments. Silent mutations were sequentially introduced in codons 600−602, 617−619, 724−725, 759−760, and 777−779 (Plg numbering) to engineer five unique restriction sites: *Pst*I, *Avr*II, *Sac*I, *Spe*I, and *Xho*I, respectively. Mutagenesis was performed by SOE-PCR (*32*) using the mutagenic oligonucleotides listed in Table 1A and the vector-specific primers LJ006 (5′-ATG-GTT-GTT-GTC-ATT-GTC-GGC-GCA) and LJ212 (5′-ATG-GGG-TTT-TGC-TAA-ACA-ACT-TTC) for reamplification of the assembled DNA product after primerless PCR reaction. The sequence of the resulting phage vector Fmyc-μPlg-5RS was confirmed by automated DNA sequencing using the Cy5 Autoread sequencing kit (Pharmacia).

Construction of Micro-Plasminogen Mutants on Phage. In total, 9 μPlg mutants were constructed in which a single amino acid residue was converted to alanine. Five μPlg mutants [μPlg(H569A), μPlg(D660A), μPlg(Y672A), μPlg(R712A), and μPlg(R719A)] were assembled by SOE-PCR using the Fmyc-μPlg-5RS vector as DNA template, the mutagenic oligonucleotides listed in Table 1B, and the vector-specific primers LJ006 and LJ212. The purified DNA fragments were digested with the appropriate restriction enzymes [*Sfi*I/*Rsr*II for μPlg(H569A), *Avr*II/*Sac*I for μPlg(D660A) and μPlg(Y672A), and *Avr*II/*Xho*I for μPlg(R712A) and μPlg(R719A)], purified on agarose gels, and ligated into the corresponding restriction sites of the Fmyc-μPlg-5RS vector prior to transformation of *Escherichia coli* TG1 cells. Cassette mutagenesis was used to construct 4 additional μPlg mutants [μPlg(R610A), μPlg(K615A), μPlg(T782A), and μPlg(R789A)]. For each mutant, a pair of 5′-phosphorylated oligonucleotides (listed in Table 1C) was annealed and directly ligated in the appropriate restriction sites of the Fmyc-μPlg-5RS vector [*Pst*I/*Avr*II for μPlg(R610A) and μPlg(K615A), and *Avr*II/*Xho*I for μPlg(T782A) and μPlg(R789A)] prior to the transformation of *E. coli* TG1 cells. All DNA sequences were confirmed by sequencing, as described above.

Characterization of Micro-Plasminogen Mutants on Phage. Phage production, purification, and storage were as described previously (*21*). The level of display of each μPlg mutant on phage was studied by Western blot analysis and densitometric scanning of phage proteins (free pIII and μPlg-pIII fusion protein) as described (*21*). Activation of the phage-displayed μPlg moieties by urokinase or Sak (typically 2×10^{12} colony-forming units (cfu)/mL with 15 nM urokinase or Sak in 50 mM Tris-HCl, 140 mM NaCl, pH 7.4 (TBS) containing 0.1% BSA during 30 min at 37 °C) was monitored by following amidolytic activity toward the chromogenic substrate S-2403. The catalytic properties of the phage-displayed μPli moieties toward S-2403 were determined from the change in absorbance at 405 nm by Lineweaver−Burk analysis as previously described (*21*). The binding activity

Table 1: Synthetic Oligonucleotides for the Construction of the Fmyc-μPlg-5RS Vector (A) and the Micro-Plasminogen Mutants by SOE-PCR (B) and Cassette Mutagenesis (C)

A. Restriction site	Backward mutagenic oligonucleotide[a]	Forward mutagenic oligonucleotide
*Pst*I	GGG-TGT-TGA-CTG-CAG-CCC-ACT-GCT-TGG	CCA-AGC-AGT-GGG-CTG-CAG-TCA-ACA-CCC
*Avr*II	ACA-AGG-TCA-TCC-TAG-GTG-CAC-ACC	CCA-ATC-CAC-CGA-GCT-CTG-TGC-TGG-GC
*Sac*I	CCA-ATC-CAC-CGA-GCT-CTG-TGC-TGG-GC	GCC-CAG-CAC-AGA-GCT-CGG-TGG-ATT-GG
*Spe*I	ACA-AGG-AGT-CAC-TAG-TTG-GGG-TCT-TGG-CTG-TGC	GCA-CAG-CCA-AGA-CCC-CAA-CTA-GTG-ACT-CCT-TGT
*Xho*I	CTA-TGT-TCG-TGT-CTC-GAG-GTT-TGT-TAC-TTG-G	CCA-AGT-AAC-AAA-CCT-CGA-GAC-ACG-AAC-ATA-G

B. Mutation	Backward mutagenic oligonucleotide	Forward mutagenic oligonucleotide
H569A[b]	AGG-GGG-GTG-TGT-GGC-CGC-CCC-ACA-TTC-CTG-GCC-CTG-GC	GCC-AGG-GCC-AGG-AAT-GTG-GGG-CGG-CCA-CAC-ACC-CCC-CT
D660A	GCC-GTC-ATC-ACT-GCC-AAA-GTA-ATC-CC	GGG-ATT-ACT-TTG-GCA-GTG-ATG-ACG-GC
Y672A	GCC-ATC-CCC-AAA-TGC-TGT-GGT-CGC-CGA-CCG-G	CCG-GTC-GGC-GAC-CAC-AGC-ATT-TGG-GGA-TGG-C
R712A	AAT-AAA-GTG-TGC-AAT-GCC-TAT-GAG-TTT-CTG-AAT-GGA-AG	CTT-CCA-TTC-AGA-AAC-TCA-TAG-GCA-TTG-CAC-ACT-TTA-TT
R719A	ATG-AGT-TTC-TGA-ATG-GAG-CTG-TCC-AAT-CCA-CCG	CGG-TGG-ATT-GGA-CAG-CTC-CAT-TCA-GAA-ACT-CAT

C. Mutation	Mutagenic cassette
R610A	p-GCC-CAC-TGC-TTG-GAG-AAG-TCC-CCA-GCG-CCT-TCA-TCC-TAC-AAG-GTC-ATC[c]
	p-CTA-GGA-TGA-CCT-TGT-AGG-ATG-AAG-GCG-CTG-GGG-ACT-TCT-CCA-AGC-AGT-GGG-CTG-CA
K615A	p-GCC-CAC-TGC-TTG-GAG-AAG-TCC-CCA-AGG-CCT-TCA-TCC-TAC-GCG-GTC-ATC
	p-CTA-GGA-TGA-CCG-CGT-AGG-ATG-AAG-GCC-TTG-GGG-ACT-TCT-CCA-AGC-AGT-GGG-CTG-CA
T782A	p-TCG-AGG-TTT-GTT-GAG-TGG-ATT-GAG-GGA-GTG-ATG-AGA-AAT-AAT-GC
	p-GGC-CGC-ATT-ATT-TCT-CAT-CAC-TCC-CTC-AAT-CCA-CTC-AAC-AAA-CC
R789A	p-TCG-AGG-TTT-GTT-ACT-TGG-ATT-GAG-GGA-GTG-ATG-GCA-AAT-AAT-GC
	p-GGC-CGC-ATT-ATT-TGC-CAT-CAC-TCC-CTC-AAT-CCA-AGT-AAC-AAA-CC

[a] Oligonucleotide sequence from 5′ to 3′ ends. [b] Single-letter codes for amino acids: A, Ala; H, His; D, Asp; Y, Tyr; R, Arg; T, Thr; K, Lys; and numbering according to the sequence of full-length human plasminogen. [c] p: phosphorylated oligonucleotide at 5′ end.

of the phage-displayed μPli moieties toward Sak was evaluated by phage-ELISA. Briefly, Sak (10 μg/mL in TBS) was coated overnight in high-binding microtiter wells (Costar) at 4 °C. After blocking with TBS containing 2% skim milk (1 h at 37 °C), the wells were incubated for 2 h with a 2-fold dilution series of each phage-displayed μPli moiety (starting with a phage input of 1×10^{10} cfu). After washing with TBS containing 0.1% Tween-20, bound phages were detected with horseradish peroxidase-conjugated anti-M13 Ig and *o*-phenylene diamine dihydrochloride (OPD) as the substrate. Absorbances were measured at 492 nm after 20 min.

Soluble Expression and Purification of Recombinant Micro-Plasminogen Moieties. The genes encoding μPlg and two mutants, μPlg(S741A) and μPlg(R719A), were subcloned as *Sfi*I/*Not*I fragments into an expression vector, pHIS, similar to pHEN1 but lacking gene *III*, whereby the expression of free, soluble proteins is directed to the *E. coli* periplasm. In addition, the DNA segment encoding the c-myc tag in pHEN1 was replaced by a $(His)_6$-encoding DNA cassette. Overnight cultures were diluted 100-fold in 3 L of LB medium supplemented with carbenicillin (100 μg/mL) and glucose (0.1%). After growing for 2 h at 37 °C, induction of the P_{lac} promoter was achieved by adding 2 L of LB medium containing carbenicillin (100 μg/mL) and 1.25 mM IPTG. After 4 h of induction at 25 °C, the cells were harvested by centrifugation, resuspended in 150 mL of TBS containing 100 μM AEBSF, and disrupted by sonication (3 × 10 min) on ice. After centrifugation for 30 min at 20 000 rpm, the cleared cell lysates were filtered through a 0.45 μm filter and adjusted to pH 7.5 and to 0.5 M NaCl before loading at a flow rate of 0.12 mL/min on a 2-mL column of CNBr-activated Sepharose derivatized with 10 mg of a murine monoclonal antibody, 31E9, specific for the proteinase domain of Plg (*28*). After the 31E9 column was washed with 10 column volumes of TBS and 0.5 M NaCl and with 10 column volumes of 0.2 M glycine−HCl buffer, pH 5.0, the bound proteins were eluted with about 3 column volumes of 0.2 M glycine−HCl buffer, pH 3.0, and collected as 0.5-mL fractions that were immediately neutralized with 100 μL of 0.5 M Tris-HCl buffer, pH 8.0. The μPlg-containing fractions were pooled and stored at −20 °C until further use. The purity of the analytical preparations was evaluated by SDS−PAGE using the Phast^R system (Pharmacia) with 10% to 15% acrylamide gradient gels. Protein concentrations were measured at 280 nm, assuming a molar absorption coefficient of 42 000 M^{-1} cm^{-1} estimated from the amino acid composition (*33*) and by densitometry of Coomassie blue-stained proteins (from 0.1 to 0.5 μg) after SDS−PAGE on 12.5% acrylamide gels using a standard of native Plg as internal control.

Binding Affinity Measurements. The binding kinetics of Sak with recombinant μPli, μPli(S741A), and μPli(R719A) were studied by real-time biospecific interaction analysis using the BIAcore instrument (Pharmacia, Biosensor AB, Sweden). Briefly, the μPlg moieties were activated by treatment with urokinase (typically a 0.5-mL sample of 5 μM proenzyme with 0.1 μM urokinase for 40 min at 37 °C) and blocked with the active-site inhibitor D-Val-Phe-Lys-CH_2Cl (final concentration 0.4 mM). The buffer was exchanged with 10 mM sodium acetate buffer, pH 5.0, by passing through a PD-10 column, and the μPli samples were

diluted to 20 μg/mL before coupling on a CM-5 sensor chip (Biosensor AB) using the Amine Coupling kit. After coupling, about 2000 resonance units of μPli moieties were immobilized. Various concentrations of Sak (from 125 nM up to 5 μM) in assay buffer (10 mM HEPES, 3.4 mM EDTA, 0.15 M NaCl, and 0.005% surfactant P20, pH 7.2) were injected at a flow rate of 5 μL/min at 20 °C. Maximal binding resulted in the adsorption of 250−300 resonance units of Sak. Several cycles of regeneration of the sensor chip by injection of 15 μL of 5 mM HCl did not alter the binding properties of the immobilized μPli moieties.

Activation of Micro-Plasminogen Moieties by Urokinase. Activation of human Plg, μPlg, μPlg(S741A), and μPlg-(R719A) (final concentration 1 μM) by urokinase (final concentration 2 or 4 nM) was measured by incubation at 37 °C. The generated plasmin at different time points (from 0 to 60 min) was measured with S-2403 (final concentration 0.3 mM) at 405 nm after a 25- to 100-fold dilution of the sample. Initial activation rates (from 0 to 5 min) were obtained from plots of the concentration of generated plasmin versus the incubation time. The catalytic efficiency (k_{cat}/K_m) was calculated from the initial activation rate and the concentration of substrate and enzyme used. Plasmin generation was further monitored in time until maximal activation was obtained. At the end of the experiments, samples were removed from the incubation mixtures, incubated with human α_2-antiplasmin (final concentration 2 μM), and subjected to SDS−PAGE under reducing conditions (1% dithioerythreitol) using the Phast^R system with 10−15% acrylamide gradient gels. Staining was performed with silver nitrate. Stock solutions of μPli were obtained by activation with urokinase immobilized on CNBr-activated Sepharose. When maximal activation was obtained, the gel was removed by centrifugation. The kinetic parameters of the μPli moieties (final concentration 1.5−2.7 nM) for the hydrolysis of S-2403 (final concentration 0.05−1.0 mM in 50 mM Tris-HCl, pH 7.4 containing 38 mM NaCl and 0.01% Tween-80) were determined by Lineweaver−Burk analysis.

Interaction of Micro-Plasminogen Moieties with Staphylokinase. The time course of active site generation (from 0 to 10 min) in equimolar mixtures of μPlg moieties (0.5 μM final concentration) with Sak (10% molar excess) in 50 mM phosphate buffer, pH 7.4, containing 0.01% Tween-80 at 37 °C was monitored with S-2403 (final concentration 0.3 mM), after a 50-fold dilution of samples. In separate experiments, Pli (1% of the (μ)Plg concentration) was added before the addition of Sak. At the end of the experiments, samples were removed for SDS−PAGE under nonreducing conditions, after addition of an excess of α_2-antiplasmin as described above. Hydrolysis of Plg(S741A) (final concentration 1 μM) by equimolar mixtures of Sak and μPli or μPli-(R719A) (final concentration 0.1 μM) after incubation for 90 min at 37 °C was monitored by SDS−PAGE under reducing conditions as described above.

RESULTS

Design and Characterization of Phage-Displayed Micro-Plasminogen Mutants. Nine site-directed mutants of μPlg were designed according to a grid-type approach in which residues spanning the accessible surface of the serine proteinase domain of Plg were substituted with alanine. The spatial arrangement of the targeted residues is shown on a ribbon diagram of the modelized serine proteinase domain of Pli (Figure 1). The mutations were engineered in the type 3 Fmyc-μPlg vector which was first re-engineered such that 5 additional restriction sites were introduced in the *μPlg* gene for easy mutagenesis, cloning, and sequencing work. Like the Fmyc-μPlg vector, the new expression vector, referred to as Fmyc-μPlg-5RS, allows the display of μPlg moieties as fusion proteins with pIII on the surface of filamentous phage (*21*). Previously we have shown that anchoring of μPlg on the phage surface does not preclude zymogen activation by urokinase, Sak, or SK and that the kinetic constants of phage-displayed μPli toward S-2403 were very similar to those of soluble mini-plasmin (mPli).

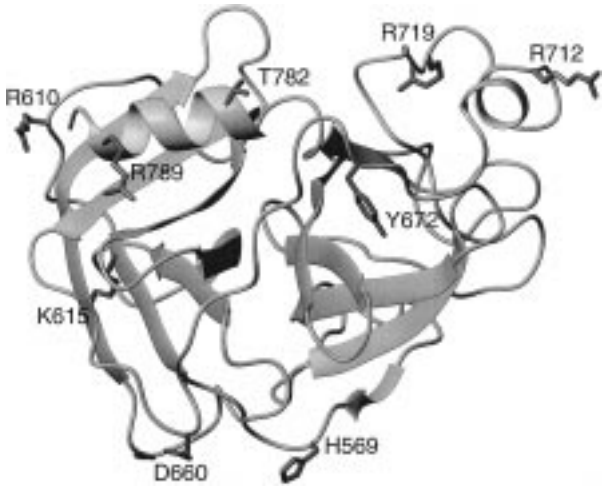

FIGURE 1: Location of the amino acid residues targeted for alanine substitution in the serine protease domain of human Pli, μPli. The modeled 3D structure of μPli is pictured as a ribbon diagram using the MolMol software (*36*). The mutated residues are numbered according to the intact Plg sequence.

Table 2: Characterization of Phage-Displayed Micro-Plasminogen Mutants

micro-plasminogen derivative	relative display level[a]	activation by urokinase	k_{cat}/K_m for S-2403 (μM^{-1} s^{-1})	relative binding affinity[b]	activation by Sak
μPlg	1	+	0.82	1	+
μPlg(H569A)	1	+	0.91	0.5	+
μPlg(R610A)	1	+	0.75	1	+
μPlg(K615A)	0.25	+	0.74	0.5	+
μPlg(D660A)	0.05	nd[c]	nd	nd	nd
μPlg(Y672A)	1	+	1.04	1	+
μPlg(R712A)	1	+	nd	0.5	+
μPlg(R719A)	1	+	0.73	<0.02	−
μPlg(T782A)	0.5	+	0.72	0.5	+
μPlg(R789A)	1	+	0.99	1	+

[a] Relative phage display level of the μPlg mutant compared to wild-type μPlg determined by densitometry of blotted phage proteins after SDS−PAGE. [b] Relative binding affinity for Sak determined by phage-ELISA of the μPlg mutant compared to wild-type μPlg. [c] nd: not determined.

Each μPlg variant was characterized according to several criteria: (i) level of display on phage, (ii) activation with urokinase and Sak, (iii) amidolytic activity toward S-2403, and (iv) binding activity to Sak. A compilation of these results is shown in Table 2. As revealed by Western blot analysis and densitometric analysis of phage proteins (data not shown), all μPlg mutants, with the exception of μPlg-(D660A) and μPlg(K615A), were expressed on phage to

Table 3: Binding Parameters of Sak to Active Site-Blocked Plasmin Moieties[a]

	binding to Sak		
plasmin moiety	k_a ($\times 10^3$ M^{-1} s^{-1})	k_d ($\times 10^{-3}$ s^{-1})	K_D ($\times 10^{-9}$ M)
Pli	330 ± 50	15 ± 0.5	46 ± 9
μPli	570 ± 100	25 ± 2.5	44 ± 3
μPli(S741A)	310 ± 18	3.3 ± 0.2	11 ± 0.2
μPli(R719A)	9 ± 2	9.1 ± 0.4	1000 ± 280

[a] The association rate constants (k_a), dissociation rate constants (k_d), and apparent dissociation constants (K_D) were determined by biospecific interaction analysis. The data represent mean ± standard deviation of three determinations.

about the same level as that of wild-type μPlg. The levels of display for μPlg(D660A) and μPlg(K615A) were significantly lower (~5% and ~25% when compared to μPlg, respectively), and the former was not further characterized. All other μPlg mutants were efficiently converted into μPli derivatives by incubation with urokinase, as judged from the generated amidolytic activity toward S-2403. The hydrolysis of S-2403 by all phage-displayed μPli variants obeyed Michaelis−Menten kinetics with k_{cat}/K_m values ranging from 0.72 to 1.0 μM^{-1} s^{-1}, in close agreement with the parameters reported for phage-displayed wild-type μPli and soluble mPli (0.66 and 0.84 μM^{-1} s^{-1}, respectively) (*21*). To identify amino acid substitutions in μPli that affect complex formation with Sak, the activated μPlg mutants were subjected to phage-ELISA, using Sak-coated wells. As shown in Table 2, only one μPli mutant, μPli(R719A), exhibits a significantly reduced binding affinity (>50-fold reduction) toward Sak. The impaired binding affinity of μPli(R719A) is compatible with the absence of amidolytic activity toward S-2403 upon incubation of phage-displayed μPli(R719A) with Sak.

Expression and Purification of Plasminogen Derivatives. To obtain free, soluble μPlg and μPlg(R719A) in sufficient amounts, the genes encoding these molecules were subcloned into a P_{lac}-controlled expression vector, pHIS, which encodes a *pelB* signal peptide for the export of recombinant products to the *E. coli* periplasm. Starting with cell lysates from 5 L cultures induced with 0.5 mM IPTG during 4 h at 25 °C, a single affinity chromatography using the immobilized monoclonal antibody, 31E9 (*28*), yielded 0.15−0.45 mg of homogeneous proteins (at least 95% pure). Another μPlg mutant that was described previously (*21*), μPlg(S741A), carrying an inactivating mutation in the catalytic site, was also obtained in soluble form with a comparable yield (0.5 mg). In the absence of urokinase, the basal amidolytic activity of μPlg and μPlg(R719A) toward S-2403 did not exceed 0.1%, which is at least 1 order of magnitude better than previously observed with their phage-attached equivalents (*21*).

Affinity of the Micro-Plasminogen Derivatives for Staphylokinase. Table 3 summarizes the association and dissociation rate constants (k_a and k_d) and apparent dissociation constants (K_D) for the binding of Sak to Pli, μPli, μPli(S741A) and μPli(R719A). The values were obtained by biospecific interaction analysis using immobilized Pli and μPli derivatives. The binding of Sak to μPli(R719A) occurred with a 24-fold lower affinity than the binding of Sak to Pli and μPli. The increased K_D value of Sak for μPli(R719A) results from a 66-fold reduction in the k_a value (9 ± 2 × 10^3 M^{-1} s^{-1} compared to 570 ± 100 × 10^3 M^{-1} s^{-1} for μPli). The K_D value of Sak for μPli(S741A) was 4-fold

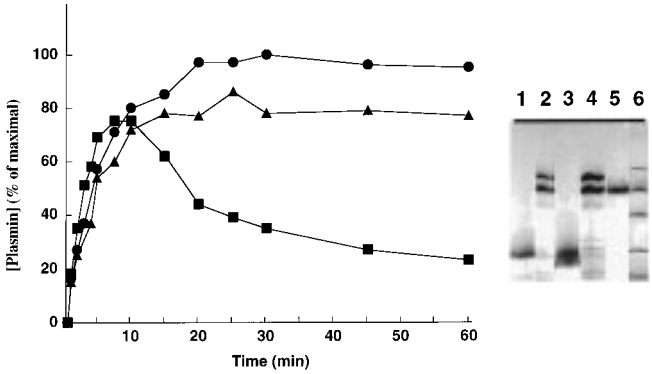

FIGURE 2: Time course of the activation of different Plg moieties (final concentration 1 μM) by urokinase (final concentration 4 nM). The Pli concentration is expressed as the percent of the concentration of native Plg (■), μPlg (●), and μPlg(R719A) (▲). The inset shows the SDS−PAGE under reducing conditions of samples taken at the start of the experiments or after the addition of excess α_2-antiplasmin at the end of the experiments [lanes 1 and 2, μPlg; lanes 3 and 4, μPlg(R719A)]. Lane 5 represents α_2-antiplasmin, and lane 6 shows a protein calibration mixture (94, 67, 45, 30, and 20 kDa).

lower than those of Pli and μPli. This result is comparable to a previous study wherein a 2-fold reduction in the K_D value was observed when Sak was complexed to Pli(S741A) instead of native Pli (*13*). The effect of the Arg719 to Ala mutation on the affinity of Plg for Sak could not be measured since, as recently reported for the Sak:Plg complex (*34*), the binding affinities of Sak for μPlg and μPlg(R719A) are too low to calculate K_D values.

Activation of the Micro-Plasminogen Derivatives by Urokinase. The catalytic efficiencies (k_{cat}/K_m) for the activation of wild-type μPlg (0.53 μM^{-1} s^{-1}) and μPlg(R719A) (0.46 μM^{-1} s^{-1}) by urokinase, as determined from the initial activation rates, were somewhat lower than those for the activation of native Plg (0.72 μM^{-1} s^{-1}) (data are mean values of experiments with 2 or 4 nM urokinase, performed with a variability of ≤10%). Prolonged incubation resulted in nearly quantitative activation, as shown by the measurement of the generated Pli activity with S-2403 (Figure 2). The addition of an excess of α_2-antiplasmin to fully activated samples yielded nearly quantitative complexation of the generated μPli and μPli(R719A) molecules with α_2-antiplasmin, as monitored by SDS−PAGE (Figure 2, insert). These results were confirmed by the total inhibition of amidolytic activity after incubation with α_2-antiplasmin. In this assay native Plg was completely converted to a two-chain species, but neither amidolytic activity nor a complex with α_2-antiplasmin was observed after the incubation of μPlg(S741A) with urokinase (data not shown). The K_m values for the hydrolysis of S-2403 (determined by linear regression analysis of the Lineweaver-Burk plots) by μPli (K_m = 90 μM; r = 0.996) and by μPli(R719A) (K_m = 110 μM; r = 0.997) were comparable to that of native plasmin (K_m = 120 μM; r = 0.999).

Interaction of the Micro-Plasmin Derivatives with Staphylokinase. In equimolar mixtures (0.5 μM) of native Plg or μPlg with Sak, active site exposure, as monitored by the hydrolysis of S-2403, was rapid and nearly quantitative (Figure 3). In contrast, no active site exposure was detected with μPlg(R719A) and μPlg(S741A). SDS−PAGE upon addition of α_2-antiplasmin confirmed active site exposure

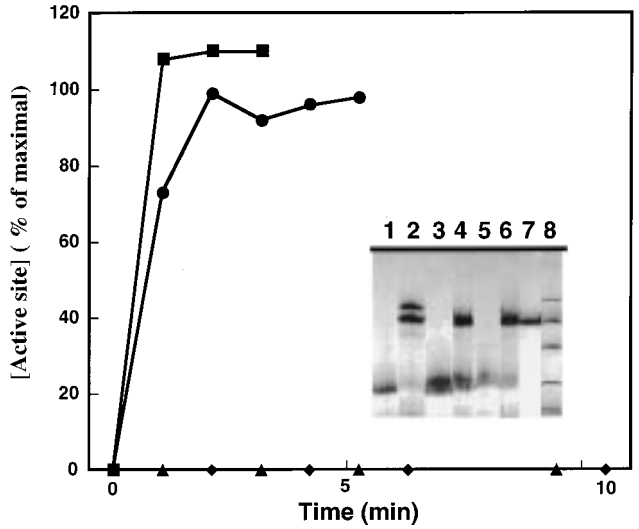

FIGURE 3: Time course of active site exposure in equimolar mixtures of Sak with native Plg (■), μPlg (●), μPlg(R719A) (▲), or μPlg(S741A) (◆). The inset shows the SDS−PAGE under reducing conditions of samples taken at the start of the experiments or after the addition of excess α_2-antiplasmin at the end of the experiments [lanes 1 and 2, μPlg; lanes 3 and 4, μPlg(R719A); lanes 5 and 6, μPlg(S741A)]. Lane 7 represents α_2-antiplasmin, and lane 8 shows a protein calibration mixture (94, 67, 45, 30, and 20 kDa).

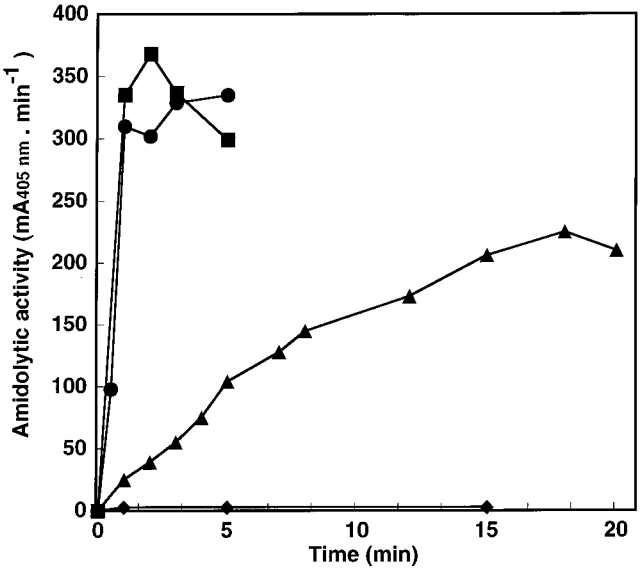

FIGURE 4: The effect of the addition of Pli (final concentration 5 nM) on the time course of the generation of amidolytic activity in equimolar mixtures (final concentration 0.5 μM) of Sak and native Plg (■), μPlg (●), μPlg(R719A) (▲) or μPlg(S741A) (◆). Amidolytic activity was measured with S-2403 (final concentration 0.3 mM) after a 50-fold dilution of the samples.

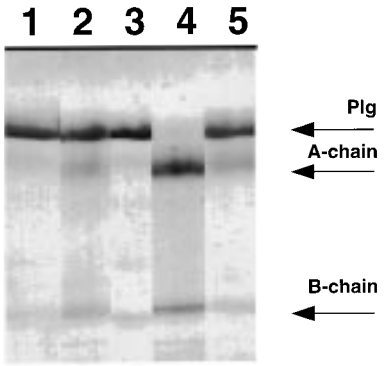

FIGURE 5: Hydrolysis of Plg(S741A) (final concentration 1 μM) by incubation at 37 °C for 90 min with preformed equimolar mixtures of Sak and μPli or μPli(R719A) (final concentration 0.1 μM), as monitored by SDS−PAGE under reducing conditions [Lane 1, Plg(S741A); lane 2, addition of μPli(R719A); lane 3, addition of Sak; lane 4, addition of Sak:μPli mixture; lane 5, addition of Sak:μPli(R719A)].

with μPlg but not with μPlg(R719A) and μPlg(S741A) (Figure 3, insert). Native Plg was also completely converted to a two-chain plasmin moiety (data not shown). Upon prolonged incubation of μPlg(R719A) and Sak at a 3-fold higher concentration (final concentration 1.5 μM), some amidolytic activity was detected, corresponding to 6% or 23% of the maximal level after 2 and 3 h, respectively (data not shown). Upon addition of 1% (molar ratio) of Pli to the Plg derivatives before the addition of Sak, active site exposure was also observed with μPlg(R719A) (although slower than with μPli) but not with μPlg(S741A), indicating that the Sak:Pli complex can activate μPlg(R719A) (Figure 4). The observed amidolytic activity indeed most likely is due to the activation of μPlg(R719A) upon selective cleavage of the Arg561−Val562 bond by the Sak:Pli complex and not due to the activator complex formation between μPli-(R719A) and Sak. This assumption is substantiated by the reduced binding affinity of μPli(R719A) for Sak as demonstrated above. Furthermore, a preformed mixture of μPli-(R719A) with Sak (final concentration 0.1 μM) did not significantly hydrolyze human Plg(S741A) (final concentration 1 μM), whereas the preformed complex with μPli did, as shown by reduced SDS−PAGE (Figure 5, lane 4). Sak alone did not hydrolyze Plg(S741A) (Figure 5, lane 3), whereas μPli(R719A) alone (Figure 5, lane 2) caused some minor cleavage, similar to that seen with its mixture with Sak (Figure 5, lane 5), but most of the substrate remained intact.

DISCUSSION

In the present study, the molecular interface of the Sak:Pli activator complex was investigated to identify amino acid residues in the serine proteinase domain of human Pli which determine its interaction with Sak. A previous structure−function study based on a "cluster charge" to alanine mutagenesis has been used to map two critical clusters of charged residues in Sak (Glu46-Lys50 and Glu65-Asp69) which mediates Sak:Pli complex formation (*14*).

Nine single alanine mutants were engineered in μPlg and expressed as fusion with the minor coat protein III on the surface of the filamentous phage. Functional phage display of these zymogens allows rapid expression and purification for the study of their biochemical properties (e.g., activation by various plasminogen activators, catalytic efficiency of proteolytic forms, and binding affinity to ligands) (*21*). A grid approach using a modeled structure of the serine proteinase domain of plasmin was used to select nine solvent-exposed residues for alanine substitution. Out of eight mutants that were studied in detail, μPlg(R719A) exhibited markedly different properties than μPlg with respect to the generation of a functional Sak:Pli complex. Incubation of phage-displayed μPlg(R719A) did not result in the generation of proteolytic activity toward S-2403, and phage-ELISA revealed a markedly reduced binding affinity of Sak to the mutant molecule. The impairment of the recognition of Sak

by phage-displayed μPlg(R719A) was not associated with a structural destabilization of the molecule since μPlg(R719A) was fully activatable with urokinase and had a comparable catalytic efficiency toward S-2403 as phage-displayed μPli and mPli. Thus, residue Arg719 in human Plg is an important determinant for the formation of a functional Sak:Pli complex. In the modeled structure of the serine proteinase domain of Pli, residue 719 is located in an extended loop in the neighborhood of the active site.

These observations were further confirmed using free, soluble μPli derivatives produced in *E. coli*. While active site exposure was rapid and quantitative in an equimolar mixture of Sak and μPlg, no activity was detected with a Sak:μPlg(R719A) mixture, as demonstrated by the absence of (i) hydrolytic activity toward S-2403 and (ii) covalent complex formation with α_2-antiplasmin. The impairment of Sak to activate μPlg(R719A) is not due to the misfolding of the zymogen since the catalytic efficiencies for the activation of μPlg and μPlg(R719A) by urokinase were similar to that for the activation of native Plg (0.53, 0.46, and 0.72 μM^{-1} s^{-1}, respectively). In addition, the K_m values for the hydrolysis of S-2403 by these activated molecules were comparable.

The Arg719 to Ala mutation is, however, not as detrimental as the inactivating active site mutation Ser741 to Ala in Plg, since a low but significant hydrolytic activity was detected after prolonged incubation (2−3 h) of Sak with μPlg(R719A). Interestingly, the large decrease of functional activity in the Sak:μPlg(R719A) complex is not proportional to the reduction of binding affinity in the complex. Indeed, the energetical contribution of residue Arg719 (−1.9 kcal/mol, as deduced from $-RT \ln(K_D \text{ mutant}/K_D \text{ wild-type})$) is only a fraction of the total binding free energy of the Sak:Pli complex (−10.0 kcal/mol). These findings indicate that, although Arg719 in Plg cannot fully account for the binding affinity of the Sak:Pli complex, it may also be required for inducing Plg activation ability in the Sak:Pli complex (e.g., by inducing a conformational change within the active site). Further mutational analysis will be required to identify other functionally important amino acids by probing adjacent residues on the modeled μPli structure.

Recently, Arg 719 was shown to be also an important determinant of the SK:Plg complex (*35*). Thus, Sak and SK, two "indirect" bacterial Plg activators with no significant homology between their primary amino acid sequences, not only share a common binding epitope on Plg (*13*), but make also critical energetical contacts with at least one common residue, Arg719, within this region. This finding suggests that, at the level of the cofactor:Pli complexes, Sak and SK may share a common mechanism to induce Plg activation ability in Pli. The elucidation of this mechanism will provide a better understanding of the thrombolytic potential of these molecules and may eventually be translated into a general concept on how to modulate the substrate specificity of Pli and other serine proteases.

ACKNOWLEDGMENT

We thank E. Demarsin and F. De Cock for assistance with zymogen purification and biospecific interaction analysis.

REFERENCES

1. Collen, D., and Lijnen, H. R. (1994) in *The molecular basis of blood diseases* (Stamatoyannopoulos, G., Nienhuis, A. W., Majerus, P. W., and Varmus, H., Eds.) pp 725−752, W. B. Saunders Company, Philadelphia.
2. Tillett, W. S., and Garner, R. L. (1933) *J. Exp. Med. 58*, 485−502.
3. Milestone, H. (1941) *J. Immunol. 42*, 109−116.
4. Lack, C. H. (1948) *Nature 161*, 559−560.
5. Lewis, J. H., and Ferguson, J. H. (1951) *Am. J. Physiol. 166*, 594−603.
6. Collen, D., and Lijnen, H. R. (1994) *Blood 84*, 680−686.
7. Reddy, K. N. N., and Markus, G. (1972) *J. Biol. Chem. 247*, 1683−1691.
8. Summaria, L., Wohl, R. C., Boreisha, I. G., and Robbins, K. C. (1982) *Biochemistry 21*, 2056−2059.
9. Cederholm-Williams, S. A., De Cock, F., Lijnen, H. R., and Collen, D. (1979) *Eur. J. Biochem. 100*, 125−132.
10. Lijnen, H. R., Van Hoef, B., De Cock, F., Okada, K., Ueshima, S., Matsuo, O., and Collen, D. (1991) *J. Biol. Chem. 266*, 11286−11832.
11. Silence, K., Collen, D., and Lijnen, H. R. (1993) *J. Biol. Chem. 268*, 9811−9816.
12. Summaria, L., and Robbins, K. C. (1976) *J. Biol. Chem. 251*, 5810−5813.
13. Lijnen, H. R., De Cock, F., Van Hoef, B., Schlott, B., and Collen, D. (1994) *Eur. J. Biochem. 224*, 143−149.
14. Silence, K., Hartmann, M., Gührs, K. H., Gase, A., Schlott, B., Collen, D., and Lijnen, H. R. (1995) *J. Biol. Chem. 270*, 27192−27198.
15. Nihalani, D., Raghava, G. P. S., and Sahni, G. (1997) *Protein Sci. 6*, 1284−1292.
16. Lin, L. F., Oeun, S., Houng, A., and Reed, G. (1996) *Biochemistry 35*, 16879−16885.
17. Davidson, D. J., Higgins, D. L., and Castellino, F. J. (1990) *Biochemistry 29*, 3585−3590.
18. Menhart, N., Hoover, G. J., McCance S. G., and Castellino, F. J. (1995) *Biochemistry 34*, 1482−1488.
19. Wang, J., Brdar, B., and Reich, E. (1995) *Protein Sci. 4*, 1758−1767.
20. Wang, J., and Reich, E. (1995) *Protein Sci. 4*, 1768−1779.
21. Lasters, I., Van Herzeele, N., Lijnen, H. R., Collen, D., and Jespers, L. (1997) *Eur. J. Biochem. 244*, 946−952.
22. Dunn, I. S. (1996) *Curr. Opin. Biotechnol. 7*, 547−553.
23. Deutz, D. G., and Mertz, E. T. (1970) *Science 170*, 1095−1096.
24. Lijnen, H. R., Van Hoef, B., and Collen, D. (1986) *Biochim. Biophys. Acta 884*, 402−408.
25. Sottrup-Jensen, L., Claeys, H., Zajdel, M., Petersen, T. E., and Magnusson, S. (1977) in *Progress in chemical fibrinolysis and thrombolysis* (Davidson, J. F., Rowan, R. M., Samama, M., and Desnoyers, P. C., Eds.) Vol. 3, pp 191−209, Raven Press, New York.
26. Lijnen, H. R., Van Hoef, B., Nelles, L., and Collen, D. (1990) *J. Biol. Chem. 265*, 5232−5236.
27. Collen, D., De Mol, M., Demarsin, E., De Cock, F., and Stassen, J. (1993) *Fibrinolysis 7*, 242−247.
28. Lijnen, H. R., Lasters, I., Verstreken, M., Collen, D., and Jespers, L. (1997) *Anal. Biochem. 248*, 211−215.
29. Claessens, M., Van Cutsem, E., Lasters, I., and Wodak, S. (1989) *Protein Eng. 2*, 335−345.
30. Desmet, J., De Maeyer, M., Hazes, B., and Lasters, I. (1992) *Nature 356*, 539−542.
31. De Maeyer, M., Desmet, J., and Lasters, I. (1997) *Folding Des. 2*, 53−66.
32. Horton, R. M., Hunt, H. D., Ho, S. N., Pullen, J. K., and Pease, L. R. (1989) *Gene 77*, 61−68.
33. Scopes, R. K. (1974) *Anal. Biochem. 59*, 277−282.
34. Sakharov, D. V., Lijnen, H. R., and Rijken, D. C. (1996) *J. Biol. Chem. 271*, 27912−27918.
35. Dawson, K. M., Marshall, J. M., Raper, R. H., Gilbert, R. J., and Ponting, C. P. (1994) *Biochemistry 33*, 12042−12047.
36. Korasi, R., Billeter, M., and Wuthrich, K. (1996) *J. Mol. Graphics 14*, 51−55.

BI972807I